Mon. Not. R. Astron. Soc. **382,** 945–950 (2007) doi:10.1111/j.1365-2966.2007.12215.x

Population III stars: hidden or disappeared?

Luca Tornatore,[1]★ Andrea Ferrara[1] and Raffaella Schneider[2]
[1]*SISSA – International School for Advanced Studies, Via Beirut 4, 34100 Trieste, Italy*
[2]*INAF – Osservatorio Astrofisico di Arcetri, Largo Enrico Fermi 5, 50125 Firenze, Italy*

Accepted 2007 July 10. Received 2007 July 5; in original form 2007 June 8

ABSTRACT

A Population III/Population II transition from massive to normal stars is predicted to occur when the metallicity of the star-forming gas crosses the critical range $Z_{\rm cr} = 10^{-5\pm1}\,{\rm Z}_{\odot}$. To investigate the cosmic implications of such a process, we use numerical simulations which follow the evolution, metal enrichment and energy deposition of both Population II and Population III stars. We find that: (i) due to inefficient heavy element transport by outflows and slow 'genetic' transmission during hierarchical growth, large fluctuations around the average metallicity arise; as a result, Population III star formation continues down to $z = 2.5$, but at a low peak rate of $10^{-5}\,{\rm M}_{\odot}\,{\rm yr}^{-1}\,{\rm Mpc}^{-3}$ occurring at $z \approx 6$ (about 10^{-4} of the Population II one); and (ii) Population III star formation proceeds in an 'inside–out' mode in which formation sites are progressively confined to the periphery of collapsed structures, where the low gas density and correspondingly long free-fall time-scales result in a very inefficient astration. These conclusions strongly encourage deep searches for pristine star formation sites at moderate ($2 < z < 5$) redshifts where metal-free stars are likely to be hidden.

Key words: galaxies: formation – intergalactic medium – cosmology: observations – cosmology: theory.

1 INTRODUCTION

The physical conditions in primordial star-forming regions appear to systematically favour the formation of very massive stars. This is due to the combined effect of the larger gas fragmentation scale and accretion rate, and the very limited opacity. On the other hand, observations of present-day stellar populations (Population I/II stars) show that stars form according to a Salpeter initial mass function (IMF) with a characteristic mass of $\approx 1\,{\rm M}_{\odot}$, below which the IMF flattens. Thus, unless the present picture of primordial star formation is lacking in some fundamental ingredients, a transition between these two modes of star formation must have occurred at some time during cosmic evolution.

What are the physical drivers of such a transition? Since the early study by Yoshii & Sabano (1980), gas metallicity has been suspected to play a key role. This idea has been later on expanded and substantiated by a number of detailed studies (Omukai 2000; Bromm et al. 2001; Schneider et al. 2002, 2003). The emerging physical interpretation states that the fragmentation properties of the collapsing clouds change as the mean metallicity of the gas increases above a critical threshold, $Z_{\rm cr} = 10^{-5\pm1}\,{\rm Z}_{\odot}$. The characteristic masses of protostellar gas clouds with $Z < Z_{\rm cr}$ are predicted to be relatively large ($>100\,{\rm M}_{\odot}$), whereas in clouds with $Z > Z_{\rm cr}$ lower characteristic masses can be formed. Within the critical metallicity range, low-mass gas clouds can form if a sufficient amount of metals is depleted on to dust grains, which provide an additional efficient cooling channel at high density (Schneider et al. 2003, 2006a; Omukai et al. 2005). According to this view, the formation of Population III stars (defined as those with $Z < Z_{\rm cr}$) is regulated by the rate at which heavy elements are produced and mixed in the gas surrounding the first star-forming regions (*chemical feedback*).

In principle, Population III stars can continue to form until late epochs, provided that gas pockets of sufficiently low metallicity can be preserved during cosmic evolution. This condition can be met for newly formed haloes that either (i) gain their gas from regions not yet polluted by outflows from nearby star-forming galaxies, or (ii) have progenitors in which star formation has not occurred or was suppressed (Ciardi & Ferrara 2005). Thus, chemical feedback can act via two physically different channels, involving either the transport of metals by outflows or in a 'genetic' form, that is, inheriting metals from the parent subhaloes (Schneider et al. 2006b).

Scannapieco, Schneider & Ferrara (2003, hereafter SSF) studied the relative importance of the outflow channel, finding that metal transport is generally inefficient; as a consequence the transition epoch is extended in time, coeval Population III and Population II star formation occurs, and Population III stars continue to form down to $z \lesssim 5$. Similar conclusions are reached by Furlanetto & Loeb (2005). Analytic models (Mackey, Bromm & Hernquist 2003) and high-resolution numerical simulations (Yoshida, Bromm & Hernquist 2004) show that if most of the early-generation stars die as pair-instability supernovae, the *volume-averaged* intergalactic

★E-mail: tornatore@oats.inaf.it

medium (IGM) metallicity will quickly reach $Z = 10^{-4}\,Z_\odot$ by $z \approx 15-20$. However, as shown by SSF and confirmed here, this condition does not guarantee a self-termination of massive Population III star formation, due to the highly inhomogeneous metal distribution.

Additional complications come from the effects of radiative feedback (Ricotti, Gnedin & Shull 2002; Machacek, Bryan & Abel 2001; Omukai & Yoshii 2003; Yoshida et al. 2003; Susa & Umemura 2006), HD chemistry (Nagakura & Omukai 2005; Greif & Bromm 2006; Johnson & Bromm 2006; Yoshida et al. 2007) and radiative transfer (Ciardi, Ferrara & Abel 2000; Kitayama et al. 2001; Ricotti, Gnedin & Shull 2001). These are generally found to be important for minihaloes ($T_{\rm vir} < 10^4$ K), or under physical conditions not relevant for this study.

Although the above studies find it difficult to rapidly suppress the formation of Population III stars, this common wisdom has to face the fact that no metal-free stars have yet been found by surveys of metal-poor stars of the Milky Way halo (Cayrel et al. 2004; Tumlinson, Venkatesan & Shull 2004; Beers & Christlieb 2005; Daigne et al. 2006; Tumlinson 2006; Salvadori, Schneider & Ferrara 2007). Alternative probes such as (i) the apparent excess in the cosmic near-infrared background (Santos, Bromm & Kamionkowski 2002; Salvaterra & Ferrara 2003; Kashlinsky et al. 2006a,b; Salvaterra et al. 2006), (ii) the equivalent width distributions of high-z Lyα emitters (Malhotra & Rhoads 2002; Dawson et al. 2004), (iii) the He II 1640 Å lines in composite spectra of Lyman break galaxies (LBGs) (Shapley et al. 2003; Nagao et al. 2005) etc., are yielding only tentative evidence for the presence of Population III stars at $z < 9$.

The question then remains: are Population III stars hidden (due to their very small statistical frequency or because they reside in yet unexplored environments) or did they disappear as a result of chemical feedback a long time ago? The aim of this letter is an attempt to address this question.

2 NUMERICAL SIMULATIONS

For this study, we have performed a set of cosmological[1] simulations using the publicly available code GADGET[2] (Springel 2005) with an improved treatment of chemical enrichment as in Tornatore et al. (2007). For this study, we have further implemented the possibility to assign different IMFs to each star-forming particle, depending on the gas metallicity. In particular, for the purpose of this work, if $Z < Z_{\rm cr}$, the adopted IMF is a Salpeter law with lower (upper) limit of $100\,{\rm M}_\odot$ ($500\,{\rm M}_\odot$); only stars in the pair-instability ($140 < M < 260\,{\rm M}_\odot$) range contribute to metal enrichment (Heger et al. 2002). If $Z \geqslant Z_{\rm cr}$, we assume that the above limits are shifted to $0.1\,{\rm M}_\odot$ ($100\,{\rm M}_\odot$), respectively; stars above $40\,{\rm M}_\odot$ end their lives as black holes swallowing their metals. In the following, we show results for $Z_{\rm cr} = 10^{-4}\,Z_\odot$. These two populations, to which we will refer to as Population III and Population II stars, respectively, differ also in their metal yield (i.e. the fraction of stellar mass transformed into metals), y, and explosion energy per unit mass of baryons going into stars, ϵ. For Population III stars, we follow Heger et al. (2002) and assume $y = 0.183$, $\epsilon = 3.5 \times 10^{16}$ erg g^{-1}; for Population II stars, we adopt a metallicity-dependent value of y taken from Woosley & Weaver (1995) and $\epsilon = 3.4 \times 10^{15}$ erg g^{-1}. Consistently with the above

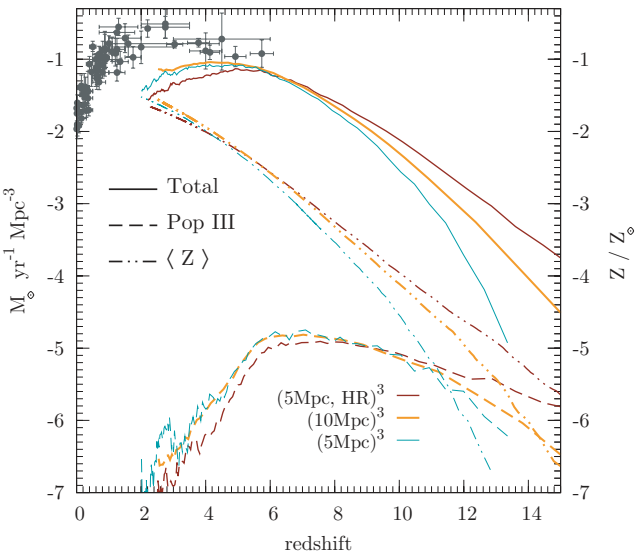

Figure 1. Predicted evolution of Population II (solid lines) and Population III (dashed lines) cosmic star formation rates, and mass-averaged metallicity (dot–dashed lines). The results of the three different simulation runs described in the text are shown for each quantity. As a reference, low-redshift measurements (points) taken from Hopkins (2004) are reported.

yields, we follow the production and transport of six different metal species, namely C, O, Mg, Si, S and Fe. In our simulations, the IMF depends on the value of the gas metallicity. Physically, the gas can be enriched by metals released by local stars or through winds powered by stars in nearby regions. Thus, the IMF is determined according to the smoothed particle hydrodynamics (SPH) value[3] rather than the intrinsic particle metallicity. For the purpose of this work, we have chosen to simulate a (comoving) volume of $L = 10\,h^{-1}$ Mpc with $N_{\rm p} = 2 \times 256^3$ (dark + baryonic) particles, corresponding to a dark matter (baryonic) particle mass of $M_{\rm p} = 3.62 \times 10^6\,h^{-1}\,{\rm M}_\odot$ ($6.83 \times 10^5\,h^{-1}\,{\rm M}_\odot$); the corresponding force resolution is 2 kpc. Our resolution does not allow to track the formation of minihaloes, whose stellar contribution remains very uncertain due to radiative feedback effects (Haiman et al. 2006; Susa & Umemura 2006; Ahn & Shapiro 2007).

The computation is initialized at $z = 99$ and carried on until $z = 2.5$. In order to check the convergence of the results, we have run two additional simulations with $L = 5\,h^{-1}$ Mpc and $N_{\rm p} = 2 \times (256^3, 128^3)$, the latter one having the same particle mass as in the reference run.

The gas photoionization and heating rates are calculated at equilibrium with a background ionizing radiation due to the combined contribution of galaxies and quasars, taken from Haardt & Madau (1996), shifted so that the intensity at 1 Ryd is $J_\nu = 0.3 \times 10^{-21}$ erg s^{-1} Hz^{-1}, in agreement with Bolton et al. (2005). Gas cools according to the cooling function given by Sutherland & Dopita (1993), corrected for both helium and hydrogen photoionization; because metal photoionization is not followed explicitly, the cooling might be somewhat overestimated. Supernova winds are treated as in the original model by Springel & Hernquist (2003); however, for simplicity and because the mass load and kinetic energy fraction are unknown parameters, we have given the winds from both

[1] Throughout this paper, we adopt a ΛCDM cosmological model with parameters $\Omega_{\rm M} = 0.26$, $\Omega_\Lambda = 0.74$, $h = 0.73$, $\Omega_{\rm b} = 0.041$, $n = 1$ and $\sigma_8 = 0.8$, in agreement with the three-year *WMAP* results (Spergel et al. 2007).
[2] www.mpa-garching.mpg.de/galform/gadget/

[3] The Z-smoothing is calculated by normalizing the kernel in a subregion of the SPH volume (here 0.2 of the SPH length), independently of the number of neighbours found.

populations an initial velocity of $v_w = 500\,\mathrm{km\,s^{-1}}$, which appears to be consistent with that derived from observations of high-z starburst galaxies (Adelberger et al. 2003; Shapley et al. 2003). Wind particles are temporarily hydrodynamically decoupled until either (i) they have moved by a travelling length $\lambda = 2$ kpc, or (ii) their density has decreased below 0.5 times the star formation density threshold ($n_\star = 0.1\,\mathrm{cm^{-3}}$). The metals are donated by star particles to the surrounding gas ones using an SPH kernel as described in Tornatore et al. (2007).

3 RESULTS

Our simulation outputs contain a wealth of useful information concerning the mode (Population III or Population II) of star formation and the source of metals associated to each particle. In addition, we can recover if heavy elements have been produced *in situ* or transported to that location by outflows.

We start the analysis of the simulation outputs by reconstructing the evolution of Population II and Population III star formation

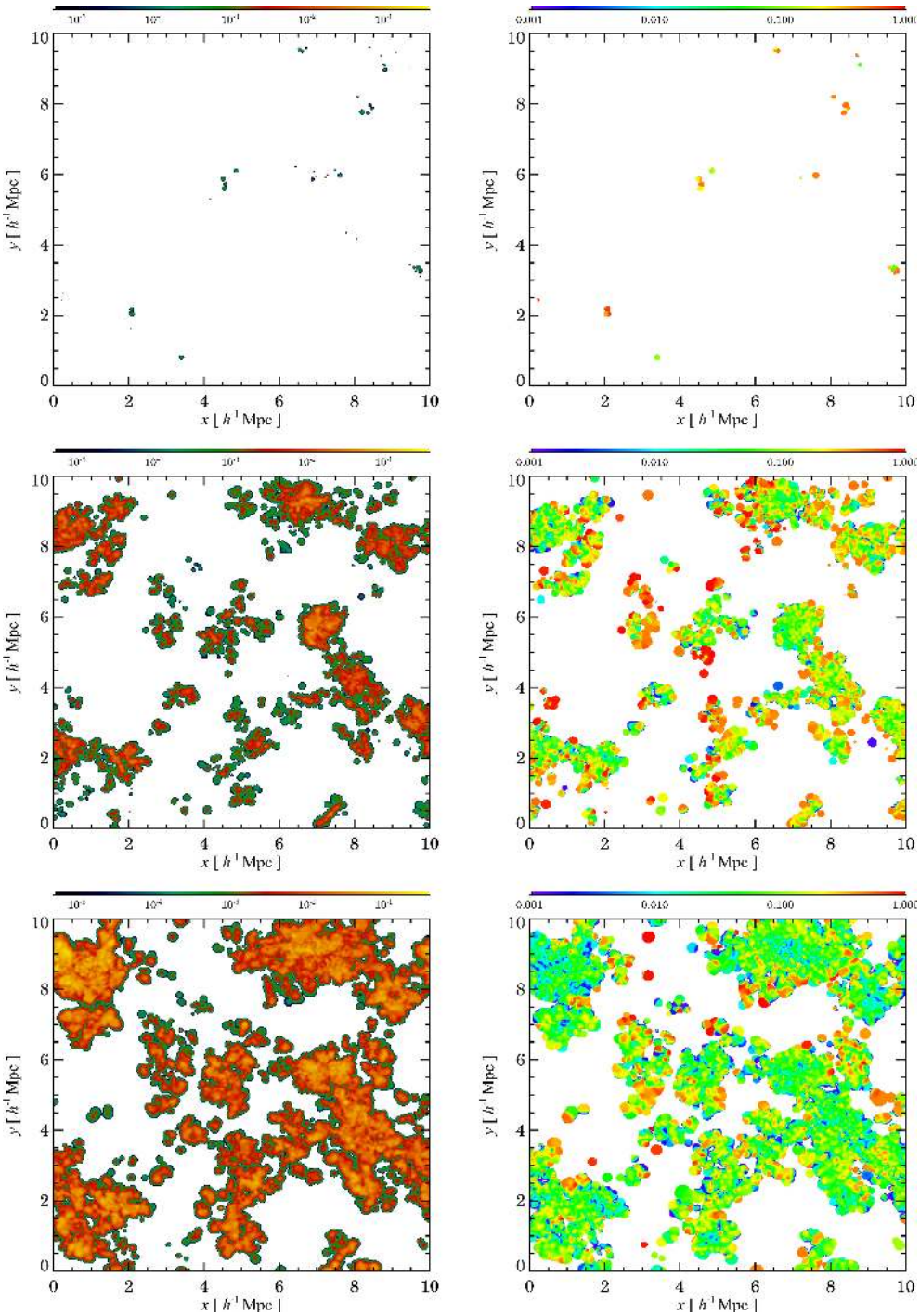

Figure 2. Maps resulting from the projection of 500-kpc-thick slices through the simulation volume of total mass-averaged metallicity, $\langle Z \rangle$ (left-hand panels) and fractional gas metallicity contributed by Population III stars, $R_3 = M_{Z,\mathrm{III}}/(M_{Z,\mathrm{III}} + M_{Z,\mathrm{II}})$ (right-hand panels) for three selected redshifts, $z = 10$, 5 and 3 from the top to bottom panel, respectively.

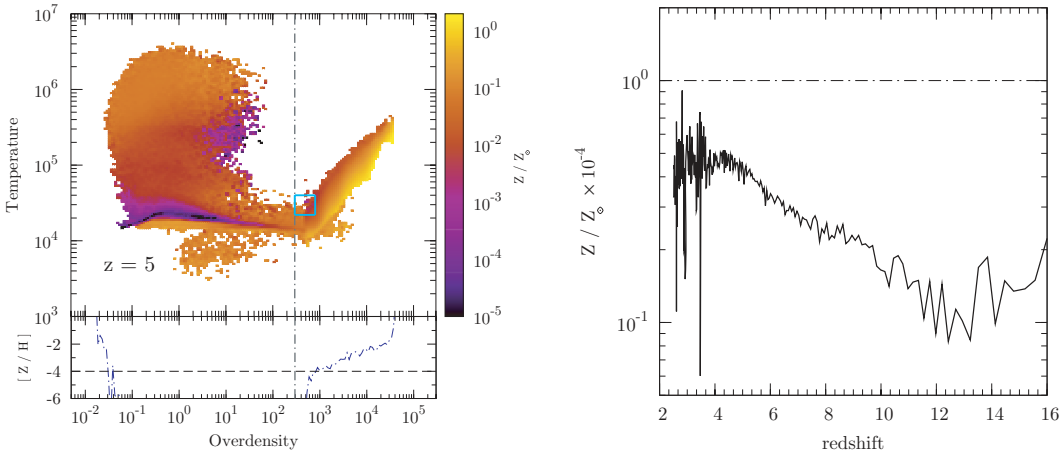

Figure 3. Left-hand panel: mass-averaged metallicity colour-coded phase diagram of the gas in the simulated volume at $z = 5$. Each pixel value represents the $\langle Z \rangle$ of the particles within a given temperature-overdensity range. The dot–dashed vertical line indicates the star formation density threshold $n_\star = 0.1$ cm^{-3}. The rectangle indicates the area in which Population III-forming particles are found. In the lower panel, we plot the minimum metallicity found in each overdensity bin (also shown with a dashed line is the value $Z = Z_{\rm cr}$); star-forming particles that have $Z < Z_{\rm cr}$ are found in the range $300 < \rho_{\rm c}/\langle\rho\rangle < 600$. Right-hand panel: mass-averaged mean metallicity of Population III-star-forming sites as a function of redshift. The dot–dashed line is the value $Z = Z_{\rm cr}$.

rates (SFRs) and the corresponding evolution of the mass-averaged metallicity, $\langle Z \rangle$, due to the dispersal of heavy elements produced by these stars. These are shown by the curves in Fig. 1. Star formation begins very early ($z \gtrsim 15$) for both populations. At these high redshifts, though, there are considerable uncertainties in the rates due to numerical resolution effects, as gathered from a comparison among the three runs reported in Fig. 1. In general, decreasing the resolution leads to an underestimate of the SFR at high redshift; smaller volumes, instead, miss the activity at later (and more easily observable) epochs. Note, however, that the scatter in the Population III/Population II SFR ratio remains <20–30 per cent independent of resolution. For this reason, we consider $L = 10\,h^{-1}$ Mpc, $N_{\rm p} = 2 \times 256^3$ as our fiducial run.

The gas mass enriched to $Z > Z_{\rm cr}$ by a single Population III star is so large that Population II stars are always the dominant star formation mode (apart from the very first event): at $z = 14$ only about 1 per cent of the stars in the universe are born in formation sites where $Z < Z_{\rm cr}$, and hence producing Population III stars. Such ratio steadily decreases reaching $\approx 10^{-4}$ at $z = 6$ and rapidly dropping afterwards.

We pause to outline two important points. First, and in agreement with previous findings by SSF and Schneider et al. (2006b), Population III stars continue to form well beyond $z = 10$, the epoch at which $\langle Z \rangle > Z_{\rm cr}$, at non-negligible rates, for example, at $z = 5$, the SFR integrated over the corresponding Hubble time would yield a Population III stellar density of $\Omega_{\rm III} \approx 2 \times 10^{-6}\ \Omega_{\rm b}$. This does not come as a surprise if we note that, due to the highly inhomogeneous nature of metal enrichment (see below), relatively pristine regions survive for several Gyr; these are the host environment for Population III formation sites. The second point to note is that, in addition to chemical feedback, the suppression of Population III star formation is also caused by the IGM photoheating due to reionization, which in our simulation occurs at $z \approx 7$. In fact, the associated increase in the Jeans (or more precisely, filtering) scale inhibits the collapse of low-mass haloes which are more likely to be relatively uncontaminated (Schneider et al. 2006) with respect to larger ones which are genetically polluted by their merging progenitors.

To make further progress, let us look at the relative spatial distribution of metals and Population III-star-forming sites. In Fig. 2, we show 500-kpc-thick slices through the simulation volume at three different redshifts $z = 3, 5$ and 10. The maps represent the spatial distribution at these three epochs of $\langle Z \rangle$ (left-hand panels) and the fractional gas metallicity contributed by Population III stars, $R_3 = M_{Z,{\rm III}}/(M_{Z,{\rm III}} + M_{Z,{\rm II}})$; by construction, $0 < R_3 < 1$. At $z = 10$, the volume-filling factor of metals is small, with only a few isolated star-forming regions. The most-active sites are rapidly making the transition to Population II star formation mode, as reflected by the fact that $R_3 \ll 1$ within the largest metal-enriched patches; it is only in the smallest and most recently polluted regions that Population III enrichment dominates ($R_3 \approx 1$). As evolution proceeds, the metal bubbles tend to grow around the most ancient star-forming sites, propagating in an inside–out fashion.[4] The metallicity structure of the bubbles is such that their interior is dominated by Population II metals, with Population III stars confined to the outermost boundary. Thus, the formation of Population III stars is forced to move away from the sites where the first generation of stars formed. In addition, it becomes less intense as it migrates away from the density peaks that harboured the first stars. The termination of the Population III era occurs when all regions with a (total) density above the star formation threshold (assumed to be $n_\star = 0.1$ cm^{-3}) reach the critical metallicity.

This evolution reverses the naively expected age–metallicity relation: at any given redshift there are (almost) metal-free stars that are *younger* than their enriched counterparts. Quantitatively, at $z = 10$ we find that of the enriched (i.e. with $Z > 0$) gas mass, a fraction of $\approx$0.26 ($\approx$0.26) is purely polluted by Population II (Population III) stars. These figures change to $\approx$0.46 ($\approx$ 0.03) at $z = 5$ and to $\approx$0.7 ($\approx$0.01) at $z = 3$. At all redshifts the remaining enriched gas has a mixed Population III/Population II composition. The overall conclusion is that below $z \approx 9$ most of the gas has been enriched only through Population II supernovae.

Fig. 3 presents the mass-averaged metallicity colour-coded phase diagram of the gas in the simulated volume. Each pixel value represents the mean temperature and $\langle Z \rangle$ of the particles within a given

[4] Note that, due to projection effects, the bubble interiors are contaminated by foreground Population III-enriched pockets.

mass-overdensity range. There we recognize the arch-shaped feature ($T \approx 10^4$ K) characterizing low-density IGM (i.e. the Lyα forest) whose thermal budget results from the balance between photoheating and adiabatic cooling. The hot, $T > 10^{4.5}$ K, tenuous (overdensity $\Delta = \rho_c/\langle\rho\rangle < 10$) phase has two distinct origins as indicated by its metallicity: (i) gas shocked by galactic outflows ($Z > 10^{-4}\,Z_\odot$), and (ii) gas virializing in forming galaxies ($Z < 10^{-4}\,Z_\odot$): galaxies forming out of this gas can potentially form Population III stars. The most relevant region of the phase plane for this study is the oblique branch found at overdensities $\Delta \gtrsim 3 \times 10^2$. Most of this dense gas has $\langle Z\rangle \gg Z_{cr}$ and is located in active regions of Population II star formation. However, a minor fraction of the gas has $\langle Z\rangle < Z_{cr}$ (region inside the rectangle in Fig. 3) and it is forming Population III stars. The Population III forming sites have densities only slightly above the critical threshold ($\Delta \approx 300$ at $z = 5$) and cool temperatures. As already pointed out, Population III star formation is progressively confined to low-density gas, that is, the periphery of collapsing structures. The right-hand panel of Fig. 3 further illustrates this point. Almost independently of redshift, Population III stars tend to form on average in regions where $\langle Z\rangle \approx 0.1\,Z_{cr}$, although a considerable spread around such value is found.

4 CONCLUSIONS

The main finding of this study is that Population III star formation can continue down to very low $z \approx 2.5$, thanks to the fact that, due to inefficient metal enrichment, pockets of almost pristine ($Z < Z_{cr}$) gas continue to exist. This confirms the results of previous semi-analytical models (SSF; Schneider et al. 2006). A general evolutionary picture emerges in which Population III star formation starts in the highest density peaks of the cosmic density field which are then polluted by their metals and turn into Population II sites, hence forcing Population III star formation to migrate towards the outer, low-density environments. The inside–out propagating 'Population III wave' stops when the environmental density has dropped below the star formation threshold, $n_\star$. Such segregation in regions of density slightly above $n_\star$ causes Population III star formation efficiency to remain low, due to the long free-fall and cooling time-scales. This is at odd with semi-analytic models which generally assume a much higher (0.01–0.1) conversion efficiency of gas to Population III stars. A more detailed comparison between numerical and semi-analytical approaches is deferred to future work. Population III stars preferentially form in regions where the mass-averaged gas metallicity is $10^{-5}\,Z_\odot$, that is, 10 per cent of the critical metallicity value adopted here. Finally, we have checked the robustness of all these results against the uncertainties in the modelling of metal transport and diffusion, adopting different numerical schemes to describe these processes, as discussed in Tornatore et al. (2007).

The above findings are quite encouraging for searches of Population III stars at moderate redshifts as it appears that rather than disappearing, these stars are hidden in the outskirts of collapsing structures. Thus, a non-negligible fraction of observable $z > 3$ objects may be powered by the radiative (Lyα emitters, LBGs: Malhotra & Rhoads 2002; SSF; Dawson et al. 2004; Jimenez et al. 2006) or mechanical (pair-instability supernovae: Scannapieco et al. 2005) input of Population III stars. On the other hand, identifying nucleosynthetic signatures of Population III stars appears extremely challenging, as only a tiny fraction (8×10^{-5}) of the baryons at $z = 3$ have been contaminated purely by Population III metals. Alternative strategies based on the detection of extremely metal-poor stars in the Galactic halo face a similar difficulty in spotting truly second-generation stars (Salvadori et al. 2007). Thus, it is likely that robust identifications of metal-free stars at high redshift would be obtained for objects characterized by large ($>10^3$ Å) Lyα equivalent widths and/or strong He II 1640 Å line. However, constraining the mass range, or even the IMF, of such stars on this basis is very difficult.

A final question remains on which physical mechanism dominates the chemical feedback: transport of metals by outflows or a 'genetic' form, that is, inheriting metals from the parent subhaloes. From the discussion above, it is clear that some fraction of the IGM is polluted by winds to high metallicity preventing it from subsequently forming Population III stars. At present, the role of the 'genetic' transmission of metals cannot be straightforwardly deduced from our study, as it requires a detailed investigation of the merging history and metallicity evolution of host haloes which we defer to future work.

ACKNOWLEDGMENTS

We are grateful to the referee, Naoki Yoshida, for his careful revision and fruitful comments. We acknowledge DAVID.[5] members for enlightening discussions. LT is grateful to Stefano Borgani for insightful suggestions.

REFERENCES

Adelberger K. L., Steidel C. C., Shapley A. E., Pettini M., 2003, ApJ, 584, 45
Ahn K., Shapiro P., 2007, MNRAS, 375, 881
Beers T.C., Christlieb N., 2005, ARA&A, 43, 531
Bolton J. S., Haehnelt M. G., Viel M., Springel V., 2005, MNRAS, 257, 1178
Bromm V., Ferrara A., Coppi P. S., Larson R. B., 2001, MNRAS, 328, 969
Cayrel R. et al., 2004, A&A, 416, 1117
Ciardi B., Ferrara A., 2005, Space Sci. Rev., 116, 625
Ciardi B., Ferrara A., Abel T., 2000, ApJ, 533, 594
Daigne F., Olive K.A., Silk J., Stoehr F., Vangioni E., 2006, ApJ, 647, 773
Dawson S. et al., 2004, ApJ, 617, 707
Furlanetto S. R., Loeb A., 2005, ApJ, 634, 1
Greif T. H., Bromm V., 2006, MNRAS, 373, 128
Haardt F., Madau P., 1996, ApJ, 461, 20
Haiman Z., Bryan G. L., 2006, ApJ, 650, 7
Heger A., Woosley S. E., 2002, ApJ, 567, 532
Jimenez R., Haiman Z., 2006, Nat, 440, 501
Johnson J. L., Bromm V., 2006, MNRAS, 366, 247
Kashlinsky A., Arendt R., Mather J. C., Moseley S. H., 2006a, ApJ, 654, 1
Kashlinsky A., Arendt R., Mather J. C., Moseley S. H., 2006b, ApJ, 654, 5
Kitayama T., Susa H., Umemura M., Ikeuchi S., 2001, MNRAS, 326, 1353
Machacek M. E., Bryan G. L., Abel T., 2001, ApJ, 548, 509
Mackey J., Bromm V., Hernquist L., 2003, ApJ, 586, 1
Malhotra S., Rhoads J. I., 2002, ApJ, 565, L71
Nagakura T., Omukai K., 2005, MNRAS, 364, 1378
Nagao T., Motohara K., Maiolino R., Marconi A., Taniguchi Y., Aoki K., Ajiki M., Shioya Y., 2005, ApJ, 631, L5
Omukai K., 2000, ApJ, 534, 809
Omukai K., Yoshii Y., 2003, ApJ, 599, 746
Omukai K., Tsuribe T., Schneider R., Ferrara A., 2005, ApJ, 626, 627
Ricotti M., Gnedin N. Y., Shull J.M., 2001, ApJ, 560, 580
Ricotti M., Gnedin N. Y., Shull J. M., 2002, ApJ, 575, 33
Salvadori S., Schneider R., Ferrara A., 2007, MNRAS, 381, 647
Salvaterra R., Ferrara A., 2003, MNRAS, 339, 973
Salvaterra R., Magliocchetti M., Ferrara A., Schneider R., 2006, MNRAS, 368, 6

[5] www.arcetri.astro.it/science/∼cosmology

Santos M. R., Bromm V., Kamionkowski M., 2002, 336, 1082
Scannapieco E., Schneider R., Ferrara A., 2003, ApJ, 589, 35 (SSF)
Scannapieco E., Madau P., Woosley S., Heger A., Ferrara A., 2005, ApJ, 633, 1031
Schneider R., Ferrara A., Natarajan P., Omukai K., 2002, ApJ, 571, 30
Schneider R., Ferrara A., Salvaterra R., Omukai K., Bromm V., 2003, Nat, 422, 869
Schneider R., Omukai K., Inoue A. K., Ferrara A., 2006a, MNRAS, 369, 1437
Schneider R., Salvaterra R., Ferrara A., Ciardi B., 2006b, MNRAS, 369, 825
Shapley A. E., Steidel C. C., Pettini M., Adelberger K. L., 2003, ApJ, 588, 65
Spergel D. N. et al., 2007, ApJS, 170, 377
Springel V., 2005, MNRAS, 364, 1105
Springel V., Hernquist L., 2003, MNRAS, 339, 312
Susa H., Umemura M., 2006, ApJ, 645, L93
Sutherland R. S., Dopita M. A., 1993, ApJS, 88, 253
Tornatore L., Borgani S., Dolag K., Matteucci F., 2007, MNRAS, in press (doi:10.1111/j.1365-2966.2007.12070.x)
Tsuribe T., Omukai K., 2006, ApJ, 642, L61
Tumlinson J., 2006, ApJ, 641, 1
Tumlinson J., Venkatesan A., Shull J. M., 2004, ApJ, 612, 602
Woosley S. E., Weaver T. A., 1995, ApJS, 101, 181
Yoshida N., Abel T., Hernquist L., Sugiyama N., 2003, ApJ, 592, 645
Yoshida N., Bromm V., Hernquist L., 2004, ApJ, 605, 579
Yoshida N., Oh P., Kitayama T., Hernquist L., 2007, ApJ, 663, 687
Yoshii Y., Sabano Y., 1980, PASJ, 32, 229

This paper has been typeset from a TEX/LATEX file prepared by the author.